Catalysis Science & Technology

PAPER

View Article Online
View Journal | View Issue

Cite this: *Catal. Sci. Technol.*, 2014, 4, 3993

Glycerol acetylation on mesoporous KIL-2 supported sulphated zirconia catalysts†

Margarita Popova,*[a] Ágnes Szegedi,[b] Alenka Ristić[c] and Nataša Novak Tušar[cd]

Received 29th April 2014,
Accepted 26th June 2014

DOI: 10.1039/c4cy00548a

www.rsc.org/catalysis

Zirconia nanomaterials were prepared by impregnation of KIL-2 type silica with 4, 8 and 12 wt.% ZrO_2 and were modified by sulphate groups in order to vary the type and strength of acidity. Samples were characterized by X-ray powder diffraction (XRD), transmission electron microscopy (TEM), and N_2 physisorption methods. Acidic properties of adsorbed pyridine were investigated by FT-IR spectroscopy. The catalytic performance of ZrKIL-2 and SO_4^{2-}/ZrKIL-2 in glycerol esterification with acetic acid was studied and compared to that of pure zirconia varieties. It was found that silica-supported zirconia samples are more active than pure zirconia ones. With increasing ZrO_2 content, KIL-2-supported catalysts showed increasing catalytic activity and selectivity in producing valuable fuel additives, di- and triacetyl glycerols. Sulphated analogues showed even higher activity and selectivity compared to non-sulphated ones due to their strong Brönsted acidity.

1. Introduction

The increasing demand for energy, chemicals and materials in our society has led research activity towards the development of green technologies, based on renewable resources.[1–3] Food waste is one of those renewable sources of carbon. Biofuels are attractive alternatives to fossil fuels due to their positive influence on the environment and the fact that they are produced from renewable sources. The production of biodiesel on an industrial scale is achieved through homogeneously catalyzed esterification. The utilization of refined oil and fats (first-generation raw materials) has led to high-cost end products and generated conflict between food and fuel production. The production of biofuels from waste has spurred on research due to the low cost of the initial raw material as well as the desire to utilize waste and solve the economic, environmental and social problems. Used cooking oil (UCO) is currently one of the most attractive feedstocks for the production of biodiesel (ref. 1–3), mostly due to its low market value. It was projected that the world biodiesel market would reach 37 billion gallons by 2016, which implied that approximately 4 billion gallons of crude glycerol would be produced.

Glycerol is a byproduct of biodiesel production of conventional and waste material sources. It emulsifies with soaps, methanol, fatty acid (FA) materials, and water to form a denser phase known as biodiesel soap stock. The FA material and methanol might be recovered from soap stock for reprocessing. The remaining mixture is generally known as glycerin, whose quality largely depends on the feedstock and the type of the employed biodiesel processing method. UCO-derived biodiesel glycerin can be refined into commercial grade (above 60 wt.% of glycerol content) to be primarily employed in non-food, non-pharma applications, based on regulatory provisions in the EU/UK. Glycerol can be converted to various valuable chemicals[4,5] through numerous routes such as etherification,[6] hydrogenolysis,[7] oxidation,[8] trans-esterification[8,9] and dehydration.[10] Besides, glycerol can be esterified with acetic acid to obtain valuable products of mono-, di- and tri-acetyl glycerol (named as MAG, DAG and TAG, respectively; Scheme 1), which have versatile industrial applications.[11] MAG and DAG can be utilized in cosmetics and medicines and as a starting monomer for the production of biodegradable polyesters;[1,11] whereas TAG can be applied as a biodiesel additive.[12] Traditionally, glycerol esterification with acetic acid is performed in the presence of mineral acids in homogeneous catalytic reactions.[11] The major drawback of homogeneous catalysis is the corrosive and harmful effects of the catalyst leading to serious technical and environmental problems. Therefore, employing heterogeneous acidic catalysts can contribute to overcoming these disadvantages.[1,11,13–16]

[a] *Institute of Organic Chemistry with Centre of Phytochemistry, Bulgarian Academy of Sciences, Acad. G. Bonchev str. bl. 9, 1113 Sofia, Bulgaria. E-mail: mpopova@orgchm.bas.bg; Fax: +359 2 8700 225; Tel: +359 2 979 39 61*
[b] *Research Centre for Natural Sciences, Hungarian Academy of Sciences, Institute of Materials and Environmental Chemistry, 1117 Budapest, Magyar tudósok körútja 2, Hungary*
[c] *National Institute of Chemistry, Hajdrihova 19, 1001 Ljubljana, Slovenia*
[d] *University of Nova Gorica, Vipavska 13, 5001 Nova Gorica, Slovenia*
† Electronic supplementary information (ESI) available. See DOI: 10.1039/c4cy00548a

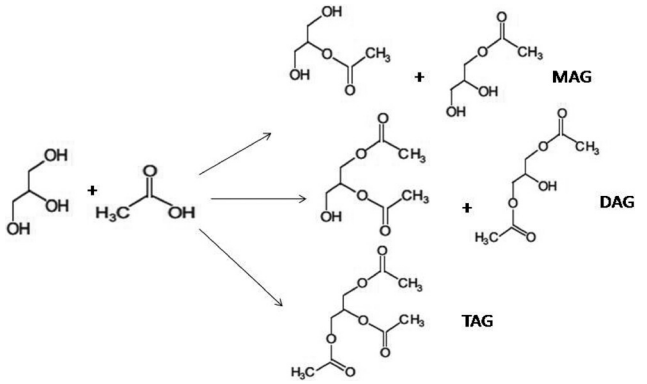

Scheme 1 Esterification of glycerol with acetic acid.

Conventional solid acidic catalysts such as mixed oxides, zeolites, Keggin-type heteropolyacids (HPAs), and sulphated zirconia (SZ) can be employed instead of classical homogeneous acids.[17–37] Among the solid acid catalysts, sulphated zirconia is one of the promising candidates because of its stability and highly acidic character.[38] SZ is widely applied in industry: *e.g.* selective isomerisation of hydrocarbons under mild conditions,[39] dehydration,[40] alkylation[41] or esterification.[42] Several studies have investigated sulphated zirconia in liquid phase esterification and transesterification reactions at temperatures higher than 373 K in excess of carboxylic acid.[42–48] Regarding the recyclability of the sulphated zirconia, in most cases the catalysts gradually lose their activity because of the leaching of sulphur during the reactions.[31] The catalytic performance of SZ strongly depends on its synthesis method, and in addition, the specific surface area of the oxide also plays an important role. There are two opportunities to enhance the catalytically active surface of SZ. One of the approaches is the deposition of zirconia on a high surface area inert support.[49,50] The other one is the preparation of high surface area oxide by means of mesopore system generation.[51–53] Mesoporous materials are a subject of great attention in the literature due to their interesting textural properties (high surface area and pore volume, uniform pore system). Mesoporous silica materials are particularly suitable carriers due to the faster mass transfer of reactants and reaction products in the nanosized pore system, making the catalytic centers easily accessible. From this point of view, the KIL-2 material with its special pore system consisting of interparticle mesoporosity is more suitable than other types of silicas with hexagonal symmetry, for instance SBA-15 and MCM-41. Pore blocking in the long, uniform channels of MCM-41 and SBA-15 during the impregnation procedure of the metal oxide precursor phase can be avoided by using the KIL-2 material.

Despite the numerous investigations, the need for a highly acidic heterogeneous catalyst for food waste upgrading and development of green technologies to obtain valuable chemicals on their basis still exists.

In the present study, the performance of ZrO_2 deposited on KIL-2 functionalized by sulphate groups in glycerol esterification with acetic acid was studied and compared to that of commercial sulphated zirconia. The influence of the textural and acidic properties on the activity and selectivity to mono-, di and triacetyl glycerol is discussed. The recyclability of the catalysts was evaluated, and selected samples were also tested in esterification of crude glycerol obtained from industrial biodiesel production.

2. Experimental

2.1. KIL-2 synthesis

In the first step, the silica source (tetraethyl orthosilicate, TEOS) and the templates were mixed with a molar composition of SiO_2 : 0.5TEA : 0.1TEAOH : $11H_2O$ to obtain a homogeneous gel.[54] The gel was aged overnight at room temperature and then dried in an oven for 24 h at 323 K. In the second step, the gel was solvothermally treated with ethanol in Teflon-lined stainless steel autoclaves at 423 K for 48 h. Removal of the template was performed by calcination at 773 K for 10 h using a ramp rate of 1 K min^{-1} in air flow.

2.2. Functionalization of KIL-2 by ZrO_2

An incipient wetness impregnation technique with $ZrCl_2$ was applied for the loading of 4, 8 and 12 wt.% metal oxide. The precursor salt was decomposed in air at 773 K for 2 hours for all samples. Samples were designated as *x*ZrKIL-2 where x = 4, 8 and 12 wt.% ZrO_2.

2.3. Functionalization of Zr/KIL-2 and ZrO_2 by SO_4^{2-} groups

Zirconia and Zr/KIL-2 samples were mixed with 10% H_2SO_4 solution (40 ml/1 g ZrO_2) at room temperature for 2 h. The suspension was dried under ambient conditions and calcined at 773 K for 3 h.

Samples were designated as SO_4^{2-}/*x*ZrKIL-2 where x = 4, 8 and 12 wt.% ZrO_2.

2.4. Characterization

The X-ray powder diffraction (XRD) patterns were recorded on a PANalytical X'Pert PRO (HTK) high-resolution diffractometer with Cu Kα_1 radiation (1.5406 Å) in the 2θ range from 5° to 60° (step size of 0.016° per 100 s) for the samples and from 10° to 90° (step size of 0.016° per 100 s) for the sample holder using a fully opened X'Celerator detector.

Nitrogen physisorption measurements were carried out at 77 K using an ASAP 2020 Micromeritics volumetric adsorption analyzer. Before the adsorption analysis, the samples were outgassed under vacuum for 2 h at 473 K in the port of the adsorption analyzer. The BET specific surface area was calculated from adsorption data in the relative pressure range of 0.06 to 0.165. The total pore volume was estimated on the basis of the amount adsorbed at a relative pressure of 0.98. The pore size distributions (PSDs) were calculated from nitrogen adsorption data using an algorithm based on the ideas of Barrett, Joyner, and Halenda (BJH).[55–57] The

mesopore diameters were determined as the maxima on the PSD for given samples.

FT-IR experiments were performed with a Nicolet Compact 640 spectrometer by the self-supported wafer technique with pyridine (Py) (7 mbar) as the probe molecule. Self-supported pellets (10 mm × 20 mm) were pressed from the samples, placed into the IR cell, heated up to 623 K in high vacuum (10^{-6} mbar) at a rate of 10 K min^{-1} and dehydrated for 1 h. Following 30-min contact with Py at 373 K the sample was evacuated subsequently at 373, 473, 573, and 673 K for 30 min. After each evacuation step a spectrum was recorded at the IR beam temperature with a resolution of 2 cm^{-1}. The spectra were normalized to 5 mg cm^{-2} weight of the wafers for comparison.

The thermogravimetric measurements were performed using a Setaram TG92 instrument with a heating rate of 5 K min^{-1} up to 873 K in air flow.

2.6. Catalytic activity measurements

Prior to the catalytic experiments, the samples were pretreated *ex situ* for 1 hour at 413 K. A batch reactor equipped with magnetic stirrer was used to perform the acetylation reaction. In a typical experiment, the reactor was charged with 2 g of glycerol and 0.1 g of catalyst, glycerol/acetic acid weight ratio = 1 : 10. The reactor was heated to the desired reaction temperature (333–373 K) for 1 hour. The analysis of the reaction products was performed using HP-GC with a WCOT FUSED SILICA 25 m × 0.25 mm COATING CP-SIL 43CB column. The catalysts were also tested with crude glycerol of industrial origin. The composition of the crude glycerol was 85.8% glycerol, 2.3% methanol and 11.9% MONG (matter organic non glycerin).

3. Results and discussion

3.1. Physico-chemical properties

XRD patterns of the studied catalysts are shown in Fig. 1. The pattern of bulk ZrO_2 shows the presence of only monoclinic phase (PDF 01-083-944). SO_4^{2-}/ZrO_2 contains a mixture of monoclinic and tetragonal ZrO_2 (PDF 01-089-6976) and zirconium disulphate tetrahydrate (PDF 01-085-0703). After the sulphate treatment, some recrystallization of ZrO_2 occurred, evidenced by the appearance of the tetragonal ZrO_2 phase and Zr sulphate.

The XRD pattern of the KIL-2 matrix at low angles indicates its disordered mesoporous nature (not shown). At high angles, ZrKIL-2 samples with 4 and 8 wt.% ZrO_2 do not show any detectable diffraction peaks that could be assigned to zirconia phases (Fig. 1B). This means either that such oxides are not present in KIL-2 samples or that their crystallite size is very small with typical dimensions of 5 nm or less and thus they are not detectable by XRD. XRD patterns show only reflections of the sample holder and one broad peak at ~23° 2θ corresponding to glass-like amorphous silicate nanoparticles.[58] However, the sample with the highest zirconia content, SO_4^{2-}/12ZrKIL-2, shows diffraction peaks that can be assigned to zirconia disulfate tetrahydrate.

Gas physisorption is extensively used for the characterisation of porous solids, particularly for the evaluation of their specific surface area, total pore volume, and pore size distribution as well as surface properties. Nitrogen adsorption isotherms of ZrKIL-2 and sulphated ZrKIL-2 materials are shown in Fig. 2, whereas structural parameters determined on the basis of these isotherms are listed in Table 1.

The commercial ZrO_2 sample has typical, relatively low surface area (5 m^2 g^{-1}) suggesting the nonporous character of the oxide. In spite of recrystallization of the ZrO_2 phase upon sulfate treatment, the specific surface area does not change significantly (6 m^2 g^{-1}). The surface area of the KIL-2 support is 664 m^2 g^{-1}, whereas supported zirconia (525–472 m^2 g^{-1}) and sulfated zirconia samples (408–306 m^2 g^{-1}) have lower surface areas.

All samples exhibit adsorption isotherms typical for KIL silicas, with a relatively narrow type IV hysteresis loop.[54,56,59,60] Higher amounts of loaded ZrO_2 on the KIL-2 support resulted in a decrease in specific surface area, pore volume and a slight increase in average pore diameter (Table 1). It can be concluded and XRD results also supported, that finely dispersed ZrO_2 nanoparticles have been homogeneously dispersed inside the KIL-2 matrix, and in contrast to impregnation with copper[59] the pore system did not change significantly. Zirconia nanoparticles are

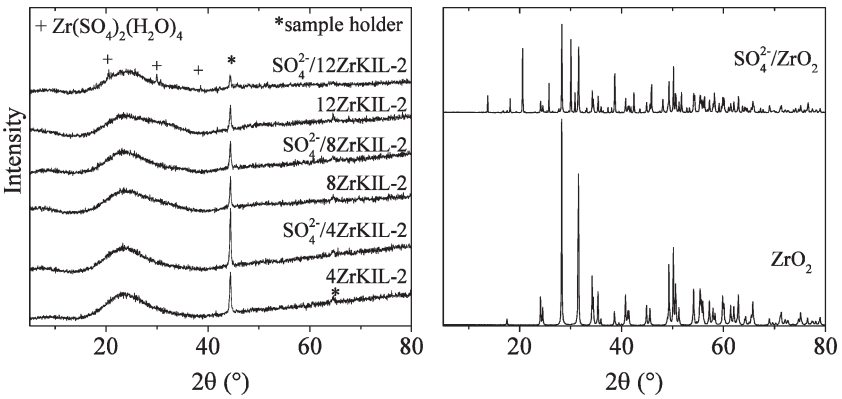

Fig. 1 XRD patterns of the studied samples.

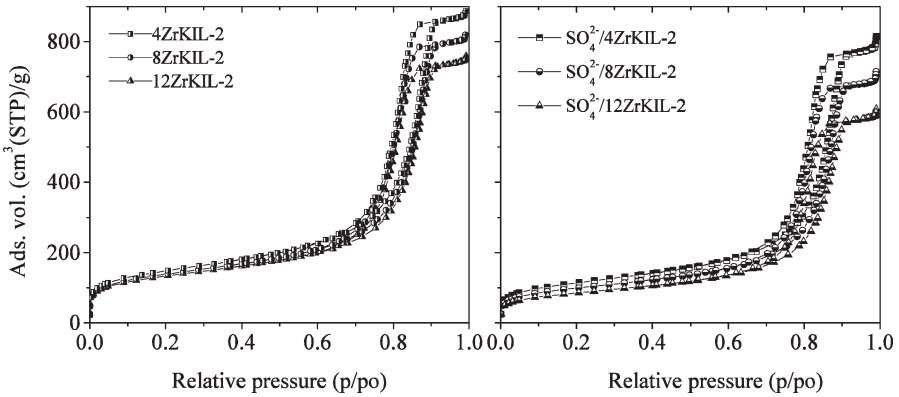

Fig. 2 Nitrogen adsorption/desorption isotherms of ZrKIL-2 catalysts and their sulfated analogues.

Table 1 Physico-chemical properties of the studied samples

Samples	S_{BET} ($m^2\ g^{-1}$)	Pore volume ($cm^3\ g^{-1}$)	Pore diameter (nm)	SO_4^{2-} (fresh cat.) (wt.%)	SO_4^{2-} (spent cat.) (wt.%)
KIL-2	664	1.43	15.2	—	—
4ZrKIL-2	525	1.34	15.7	—	—
SO_4^{2-}/4ZrKIL-2	408	1.20	16.2	2.7	2.6
$8ZrO_2$/KIL-2	494	1.24	15.7	—	—
SO_4^{2-}/8ZrKIL-2	355	1.06	16.2	5.3	5.2
12ZrKIL-2	472	1.14	15.4	—	—
SO_4^{2-}/12ZrKIL-2	306	0.90	15.7	7.4	7.2

immobilized in the silica matrix due to the interaction with the silanol groups on the surface and are not inclined to agglomerate, like copper oxide. Sulphate functionalization of ZrKIL-2 samples also led to somewhat decreased specific surface area and pore volume (Table 1). It can also be observed that sulfated ZrKIL-2 samples undergo a capillary condensation step at higher relative pressures than the ZrKIL-2 samples, indicating that larger mesopores are present in the sulfated samples. This effect can be explained by some destruction of the mesostructured pore system caused by the corrosive action of sulfuric acid, resulting in some dissolution of silica.[61]

Textural characteristics of ZrKIL-2 samples are supported by TEM investigations. Fig. 3 shows the TEM images of

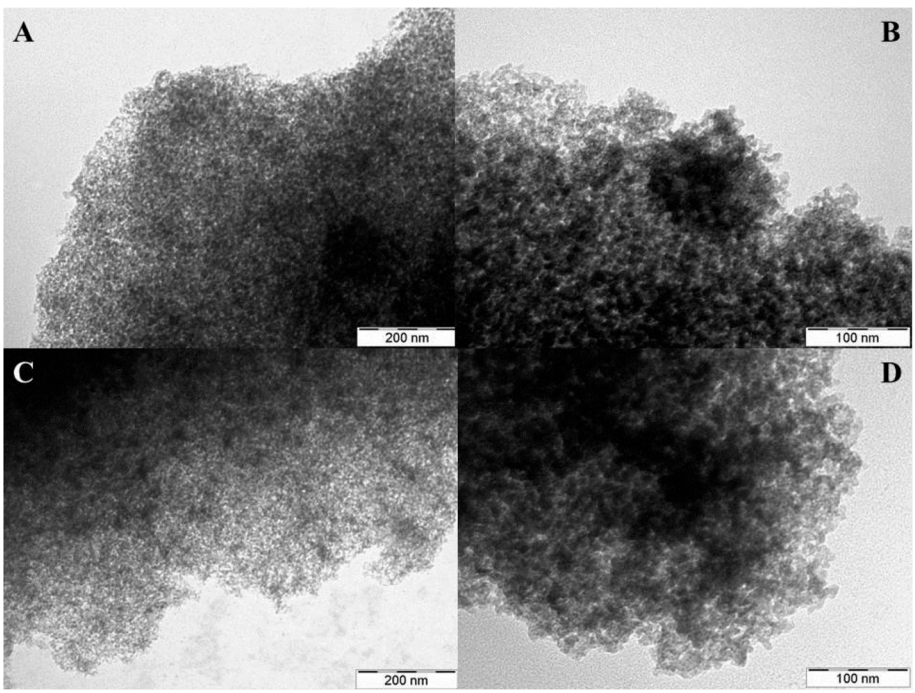

Fig. 3 TEM images of 12ZrKIL-2 (A, B) and SO_4^{2-}/12ZrKIL-2 samples (C, D).

the 12ZrKIL-2 sample and its sulphated variety. No bigger, agglomerated zirconia particles can be seen on the images, and the pore system seems to be similar upon the impregnation procedure and the sulphuric acid treatment.

3.2. Characterization by FT-IR of adsorbed pyridine

Zirconia and sulphated zirconia materials show acidic properties, *i.e.* Lewis and Brönsted acid surface sites can be distinguished. The relative amount and nature of these types of acidic species can be determined by FT-IR spectroscopic investigation of adsorbed pyridine (Py). The bands at about 1610 cm^{-1} and 1448 cm^{-1} are assigned to Py coordinated to Lewis acid sites (Py-L). The protonated Py molecules coordinated to the conjugated base of the solid Brönsted acid (Py-B) exhibit bands at 1545 cm^{-1} and 1639 cm^{-1}. The weak band at 1446 cm^{-1} appearing as a shoulder of the 1448 cm^{-1} band and the 1598 cm^{-1} band can be associated with the ring vibrations of physisorbed Py (Py-H).[62] The surface silanol groups of silica materials, such as KIL-2, are possible sites of this weak physisorption. The coordinatively unsaturated Zr ions on the surface of zirconia can act as Lewis acid sites.[63] On sulphated zirconia, the sulphate species are also Lewis acid sites; however, the presence of the latter species increases the Brönsted acid strength of hydroxyl groups on the surface of zirconia.[63] Brönsted acid sites can also be formed when zirconia–silica mixed oxides are formed.[64] The KIL-2 support contains high amount of silanol groups; therefore it is highly probable that upon impregnation with the zirconia precursor salt, Si–O–Zr bonds can be generated. FT-IR spectra of adsorbed Py on sulphated and non-sulfated ZrKIL-2 samples with 4 and 12% metal oxide contents are shown in Fig. 4. In the spectra of non-sulphated ZrKIL-2 samples, intense bands at 1448 and at 1612 cm^{-1}, characteristic of Lewis acid sites, can be observed. The weak bands at 1543 and 1639 cm^{-1} can be assigned to the Brönsted acidity of the sample. The Py is desorbed from these sites at about 473 K, indicating the weak acid strengths. Such weak Brönsted acid sites can be formed on mixed zirconia–titania/silica oxides,[64] evidencing that during the impregnation procedure zirconia reacted with the silica carrier. This is also supported by the significant intensity decrease of the 3740 cm^{-1} and 3620 cm^{-1} bands in the υ_{OH} region of the spectra (not shown) of the 12ZrKIL-2 sample compared to 4ZrKIL-2. This indicates that the amount of terminal and hydrogen bonded silanol groups decreased due to the reaction upon deposition of the zirconia phase by incipient wetness impregnation. Upon sulphate treatment, the intensity of bands, characteristic of Lewis acid sites, decreased, and Brönsted acid sites increased. However, not only the amount changed but also their strength. Py cannot be totally removed even at 673 K. This points towards the fact that after the sulphate treatment strong Brönsted acid sites can be created even on the surface of silica-supported zirconia. The S═O stretching vibration of sulphate species also appeared in the spectra of the sulphated samples at about 1350 cm^{-1} (not shown). In FT-IR spectra of sulphated zirconia, there are bands close to 1400 cm^{-1} and in the 1385–1340 cm^{-1} region.[64] The former can be associated with the S═O stretching vibration of disulphate and the latter with monosulphate species. The actual frequency of the bands depends on the sulphate coverage and the heterogeneity of the surface, but the lack of disulphate species indicates that there are no big zirconia domains or particles. According to XRD results the particle size of zirconia is below 5 nm, and these domains are probably too small to allow the disulphate formation. This fact is also supported by the Zr/SO_4^{2-} ratio of the samples (Table 1) being around 1.5–1.6 for all samples.

3.3. Catalytic activity for glycerol esterification with acetic acid

All samples were tested in glycerol esterification with acetic acid in the liquid phase and the activity and the selectivity to MAG, DAG and TAG are presented in Tables 2 and 3. The applied excess of acetic acid (glycerol : acetic acid = 1 : 10) decreases the time required to reach the reaction equilibrium and provides more acetylating agent, needed for the formation of DAG and TAG.[12,14,31] The reaction reached its maximum conversion after 2 h reaction time. The catalytic properties of

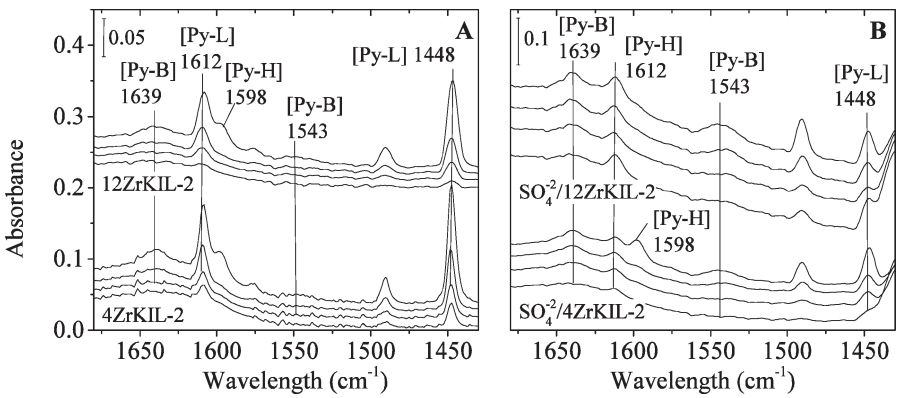

Fig. 4 FT-IR spectra of adsorbed pyridine on non-sulfated (A) and sulphated (B) ZrKIL-2 samples with 4 and 12 wt.% of zirconia. Self-supported pellets were pretreated at 623 K in vacuum and contacted with Py (7 mbar) for 30 min. Spectra were collected after Py desorption at 373, 473, 573, and 673 K for 30 min, shown from top to bottom for each sample.

Table 2 Selectivity to monoacetylglycerols, diacetylglycerols and triacetylglycerol of ZrKIL-2 and SO_4^{2-}/ZrKIL-2 samples

	333 K				353 K				373 K			
	Conv.	MAG	DAG	TAG	Conv.	MAG	DAG	TAG	Conv.	MAG	DAG	TAG
Catalysts	wt.%				wt.%				wt.%			
ZrO_2	0	0	0	0	16.4	92.1	7.9	0	73.3	69.8	24.1	4.5
SO_4^{2-}/ZrO_2	13.7	87.8	12.2	0	90.0	55.6	32.1	12.3	95.0	10.7	76.1	13.2
4ZrKIL-2	0	0	0	0	15.8	93.3	6.7	0	48.1	75.9	12.1	12.1
SO_4^{2-}/4ZrKIL-2	13.7	84.6	15.4	0	74.4	66.2	24.3	9.5	100	23	58	19
8ZrKIL-2	0	0	0	0	26.4	86.7	13.3	0	70.3	63.4	26.8	9.9
SO_4^{2-}/8ZrKIL-2	25.7	73.1	19.2	7.7	94.7	51.6	34.7	13.7	100	11	69	21
12ZrKIL-2	0	0	0	0	35.7	84.3	13.2	2.5	80.9	60.9	27.9	11.1
SO_4^{2-}/12ZrKIL-2	41.6	77.3	17.1	5.5	100	32.3	49.0	18.7	100	2.7	77.1	20.1

Table 3 Esterification of crude glycerol with acetic acid on the selected samples

	353 K				373 K			
		MAG	DAG	TAG		MAG	DAG	TAG
Catalysts	Conv. %	wt.%			Conv. %	wt.%		
SO_4^{2-}/12ZrKIL-2 glycerol : acetic acid = 1 : 10	44.2	77.8	17.8	4.4	91.1	63.7	26.4	9.9
SO_4^{2-}/12ZrKIL-2 glycerol : acetic acid = 1 : 15	68.2	40.3	42.4	17.1	79.6	12.2	67.3	20.5
SO_4^{2+}/ZrO_2 glycerol : acetic acid = 1 : 10	23.4	63.4	26.8	9.8	56.6	63.2	27.6	9.2

KIL-2 supported ZrO_2 and their sulphated varieties were compared to those of commercial bulk ZrO_2 and its sulphated ZrO_2 analogue, respectively (Tables 2 and 3). At lower temperature (333 K), ZrKIL-2 samples do not show any catalytic activity; however their sulphated analogues can convert glycerol mainly to MAG. At this low temperature, the selectivity to MAG was 87.8%, 73.1% and 77.3% for SO_4^{2-}/4ZrKIL-2, SO_4^{2-}/8ZrKIL-2 and SO_4^{2-}/12ZrKIL-2, respectively. The activity increases with increasing ZrO_2 content (from 14 to 42%). Increasing the reaction temperature (from 333 K to 353 K and then to 373 K) results in higher catalytic activity for both ZrKIL-2 and sulphated ZrKIL-2 samples. The DAG and TAG yields increased with the increasing amount of available active sites, *i.e.* Lewis and Brönsted acid sites. At low temperature the activity of the SO_4^{2-}/4ZrKIL-2 catalyst is similar to that of bulk ZrO_2, namely, 15.8% *vs.* 16.4%. A significant increase of yields of DAG and TAG can be observed for sulphated ZrKIL-2 samples, reaching 97.2% for SO_4^{2-}/12ZrKIL-2. This effect can be explained by the presence of SO_4^{2-} anions on the surface, increasing the Brönsted acidity of the catalyst (see Fig. 4, FT-IR results) and enhancing the surface interactions between the acylium moiety of the acetic acid and the OH^- anion of glycerol.[15] The acylium ion formation rate on the catalyst surface represents the determining step during the acetylation reaction. The acid site–acetic acid complex can facilitate the approach of glycerol molecules rather than that of other acetic acid molecules and this complex can be susceptible to multiple nucleophilic attacks of the hydroxyl groups of glycerol.[16,62] The consecutive acetylation reactions are highly endothermic with temperature-dependent selectivity, which explains the formation of the MAG product mainly at low temperatures (around 333 K).[15,31,65,66] However, the observation that sulphated ZrKIL-2 catalysts, independently of the amount of ZrO_2, which presented higher activity in comparison to the non-sulphated ones, indicates that their formation is rather governed by the acidic strength of the catalyst than by the number of active sites.[67,68] Comparing the catalytic activity of ZrKIL-2 samples to that of bulk ZrO_2 it can be seen that 4ZrKIL-2 shows similar catalytic activity to crystalline ZrO_2, and the catalysts with increasing supported zirconia content exceed it. It can also be concluded that even small amounts of strong acidic sites are enough to achieve high conversion and high selectivity to valuable products. The sulphate treatment resulted in higher DAG and TAG yields for all ZrKIL-2 catalysts than bulk sulphated zirconia. The weight losses due to SO_4^{2-} degradation calculated by the TG experiments are:7.4 wt.%, 5.3 wt.% and 2.7 wt.% for SO_4^{2-}/12ZrKIL-2, SO_4^{2-}/8ZrKIL-2 and SO_4^{2-}/4ZrKIL-2, respectively (Table 1). The higher dispersion of ZrO_2 in SO_4^{2-}/12ZrKIL-2 resulted in a higher amount of formed SO_4^{2-}. As evidenced also by FT-IR results on the highly dispersed zirconia phase sulphate groups can be found relatively separated and therefore can more easily be accessed by the reactants. Moreover, the diffusion of the products is also facilitated.

After the reaction, the catalyst was separated from the reaction mixture by centrifugation and dried at 373 K before application in the next run. The conversion and selectivity values for the three runs of the reaction on SO_4^{2-}/12ZrKIL-2 are shown in Fig. 5. The catalyst was stable in the consecutive procedures and no significant change could be observed in the activity and selectivity. The XRD and N_2 physisorption data of the spent catalysts also do not show significant loss of structure ordering (ESI†) and surface functionality. Generally, sulphate leaching is the main reason for the deactivation of SZ. The registered SO_4^{2-} weight loss of the spent catalysts does not show significant decrease compared to the fresh samples (Table 1).

SO_4^{2-}/ZrO_2 and SO_4^{2-}/12ZrKIL-2 were additionally tested in acetylation of crude glycerol obtained from industrial

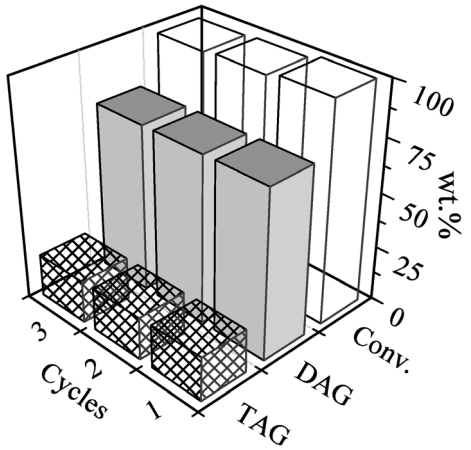

Fig. 5 Catalytic stability of the SO_4^{2-}/12ZrKIL-2 catalyst in glycerol esterification at 373 K.

biodiesel production. The applied crude glycerol contains 85.8% glycerol, 2.3% methanol and 11.9% MONG (matter organic non glycerin). Data are summarized in Table 3. Impurities of crude glycerol did not significantly influence the catalytic activity, but strongly affected the selectivity on both studied catalysts. With this raw material, SO_4^{2-}/12ZrKIL-2 also showed better activity and selectivity to DAG and TAG than SO_4^{2-}/ZrO_2. Selectivity was probably influenced by the change in glycerol/acetic acid ratio when crude glycerol was applied because acetic acid could react with methanol and other organic impurities as well (Table 3).

This assumption was proven by the catalytic experiment on SO_4^{2-}/12ZrKIL-2 with glycerol : acetic acid ratio = 15 (Table 3). Under the applied conditions the catalyst showed higher conversion and much higher selectivity to DAG and TAG (87.8 wt.% at 373 K). Wang *et al.*[69] detected similar selectivity to valuable products (97.93%) for the SO_4^{2-}/ZrO_2 catalyst but the amount of the catalyst for the quality of glycerin is 5 wt%, whereas in our experiment this value is 1 wt.% for SO_4^{2-}/12ZrKIL-2. This result could be explained by the improved zirconia dispersion on SO_4^{2-}/12ZrKIL-2, which leads to better catalytic performance.

4. Conclusion

Sulphated ZrO_2-modified mesoporous KIL-2 silicas were prepared and investigated as catalysts in glycerol esterification with acetic acid. The catalysts show high catalytic activity and selectivity to di- and tri-acetylglycerols. The sulphated 12 wt.% ZrO_2 containing KIL-2 catalyst appears more efficient than commercial sulphated zirconia in the esterification reaction. Investigation of acidic properties of the catalysts revealed that even a small amount of the highly dispersed zirconia phase is enough to provide sufficient amounts of catalytically active sites with strong acidity. The high dispersion of the zirconia phase on the silica carrier makes it possible to separate the active sites facilitating the adsorption of reactants and desorption of products.

Acknowledgements

Financial support from the project ДНТС/СЛОВЕНИЯ 01/6, COST action TD1203, the SRA program P1-0021 and by the Bulgarian-Hungarian Inter-Academic Exchange Agreement is greatly acknowledged.

References

1 R Luque, J Campelo and J Clark, *Handbook of biofuels production: Processes and technologies*, Woodhead Publishing Series in Energy No. 15, 2013.
2 C. S. K. Lin, L. A. Pfaltzgraff, L. Herrero-Davila, E. B. Mubofu, S. Abderrahim, J. H. Clark, A. Koutinas, N. Kopsahelis, K. Stamatelatou, F. Dickson, S. Thankappan, Z. Mohamed, R. Brocklesby and R. Luque, *Energy Environ. Sci.*, 2013, **6**, 426.
3 J. H. Clark, V. Budarin, T. Dugmore and R. Luque, *Catal. Commun.*, 2008, **9**, 1709.
4 D. J. Macquarrie, V. Strelko, M. S. Khayoon and B. H. Hameed, *Appl. Catal., A*, 2012, **433–434**, 152.
5 C. H. Zhou, H. Zhao, D. S Tong, L. M. Wu and W. H. Yu, *Catalysis Reviews: Science and Engineering*, 2013, **55**, 369.
6 K. Wilson, A. F. Lee, D. J. Macquarrie and J. H. Clark, *Appl. Catal., A*, 2002, **228**, 127.
7 R. van Grieken, J. A. Melero and G. Morales, *Appl. Catal., A*, 2005, **289**, 143.
8 D. Liang, J. Gao, H. Sun, P. Chen, Z. Hou and X. Zheng, *Appl. Catal., B*, 2011, **106**, 423.
9 S. Shylesh, S. Sharma, S. P. Mirajkar and A. P. Singh, *J. Mol. Catal.*, 2004, **212**, 219.
10 M. Trejda, K. Stawicka and M. Ziolek, *Appl. Catal., B*, 2011, **103**, 404.
11 C.-H. Zhou, J. N. Beltramini, Y.-X. Fana and G. Q. Lu, *Chem. Soc. Rev.*, 2008, **37**, 527.
12 M. L. Testa, V. La Parola, L. F. Liotta and A. M. Venezia, *J. Mol. Catal.*, 2013, **367**, 69.
13 J. A. Sánchez, D. L. Hernández, J. A. Moreno, F. Mondragón and J. J. Fernández, *Appl. Catal., A*, 2011, **405**, 55.
14 K. Jagadeeswaraiah, M. Balaraju, P. S. Sai Prasad and N. Lingaia, *Appl. Catal., A*, 2010, **386**, 166.
15 M. S. Khayoon and B. H. Hameed, *Bioresour. Technol.*, 2011, **102**, 9229.
16 T. Borrego, M. Andrade, M. L. Pinto, A. Rosa Silva, A. P. Carvalho, J. Rocha, C. Freire and J. Pires, *J. Colloid Interface Sci.*, 2010, **344**, 603.
17 D. Pérez-Quintanilla, A. Sánchez, I. del Hierro, M. Fajardo and I. Sierra, *J. Colloid Interface Sci.*, 2007, **313**, 551.
18 E. Li, Z. P. Xu and V. Rudolph, *Appl. Catal., B*, 2009, **88**, 42.
19 M. S. Khayoon, M. A. Olutoye and B. H. Hameed, *Bioresour. Technol.*, 2012, **111**, 175.
20 A. Corma, G. W. Huber, L. Sauvanaud and P. O'Connor, *J. Catal.*, 2008, **257**, 163.
21 H. Liu, L. Su, F. Liu, C. Li and U. U. Solomon, *Appl. Catal., B*, 2011, **106**, 550.

22 K. Pathak, K. M. Reddy, N. N. Bakhshi and A. K. Dalai, *Appl. Catal., A*, 2010, **372**, 224.
23 F. A. F. Frusteri, G. Bonura, C. Cannilla, L. Spadaro and O. Di Blasi, *Appl. Catal., A*, 2009, **367**, 77.
24 A. Bienholz, H. Hofmann and P. Claus, *Appl. Catal., A*, 2011, **391**, 153.
25 D. Liang, J. Gao, H. Sun, P. Chen, Z. Hou and X. Zheng, *Appl. Catal., B*, 2011, **106**, 423.
26 J. Li and T. Wang, *Chem. Eng. Process.: Process Intensif.*, 2010, **49**, 530.
27 E. Yoda and A. Ootawa, *Appl. Catal., A*, 2009, **360**, 66.
28 P. Ferreira, I. M. Fonseca, A. M. Ramos, J. Vital and J. E. Castanheiro, *Appl. Catal., B*, 2009, **91**, 416.
29 P. C. Smith, Y. Ngothai, Q. Dzuy Nguyen and B. K. O'Neill, *Renewable Energy*, 2010, **35**, 1145.
30 M. Balaraju, P. Nikhitha, K. Jagadeeswaraiah, K. Srilatha, P. S. Sai Prasad and N. Lingaiah, *Fuel Process. Technol.*, 2010, **91**, 249.
31 I. Dosuna-Rodriguez, C. Adriany and E. M. Gaigneaux, *Catal. Today*, 2011, **167**, 56.
32 P. Ferreira, I. M. Fonseca, A. M. Ramos, J. Vital and J. E. Castanheiro, *Catal. Commun.*, 2009, **10**, 481.
33 P. Ferreira, I. M. Fonseca, A. M. Ramos, J. Vital and J. E. Castanheiro, *Catal. Commun.*, 2011, **12**, 573.
34 W. Li, K. Oshihara and W. Ueda, *Appl. Catal., A*, 1999, **182**, 357.
35 B. M. Devassy, G. V. Shanbhag and S. B. Halligudi, *J. Mol. Catal. A: Chem.*, 2006, **247**, 162.
36 P. Sharma and A. Patel, *Appl. Surf. Sci.*, 2009, **255**, 7635.
37 R. Luque and J. H. Clark, *ChemCatChem*, 2011, **3**, 594.
38 G. D. Yadav and J. J. Nair, *Microporous Mesoporous Mater.*, 1999, **33**, 1.
39 A. Sassi and J. Sommer, *Appl. Catal., A*, 1999, **188**, 155.
40 S. Chokkaram and B. H. Davis, *J. Mol. Catal. A: Chem.*, 1997, **118**, 89.
41 R. B. Gore and W. J. Thomson, *Appl. Catal., A*, 1998, **168**, 23.
42 D. E. López, J. G. Goodwin Jr., D. Bruce and S. Furuta, *Appl. Catal., A*, 2008, **339**, 76.
43 T. A. Peters, N. E. Benes, A. Holmen and J. T. F. Keurentjes, *Appl. Catal., A*, 2006, **297**, 182.
44 A. A. Kiss, A. C. Dimian and G. Rothenberg, *Adv. Synth. Catal.*, 2006, **348**, 7.
45 J. Ni and F. C. Meunier, *Appl. Catal., A*, 2007, **333**, 122.
46 K. Suwannakarn, E. Lotero, J. G. Goodwin and C. Lu, *J. Catal.*, 2008, **255**, 279.
47 J. Jitputti, B. Kitiyanan, P. Rangsunvigi, K. Bunyakiat, L. Attanatho and P. Jenvanitpanjakul, *Chem. Eng. J.*, 2006, **116**, 61.
48 C. M. Garcia, S. Teixeira, L. L. Marciniuk and U. Schuchardt, *Bioresour. Technol.*, 2008, **99**, 6608.
49 M. D. Gracia, A. M. Balu, J. M. Campelo, R. Luque, J. M. Marinas and A. A. Romero, *Appl. Catal., A*, 2009, **371**, 85.
50 J. Iglesias, M. D. Gracia, R. Luque, A. A. Romero and J. A. Melero, *ChemCatChem*, 2012, **4**, 379.
51 V. G. Deshmane and Y. G. Adewuyi, *Microporous Mesoporous Mater.*, 2012, **148**, 88.
52 M. Chidambaram, C. Venkatesan and A. P. Singh, *Appl. Catal., A*, 2006, **310**, 79.
53 W. Hua, Y. Yue and Z. Gao, *J. Mol. Catal.*, 2001, **170**, 195.
54 N. Novak Tušar, A. Ristić, G. Mali, M. Mazaj, I. Arčon, D. Arčon, V. Kaučič and N. Zabukovec Logar, *Chem. – Eur. J.*, 2010, **16**, 5783.
55 S. Brunauer, P. H. Emmett and E. Teller, *J. Am. Chem. Soc.*, 1938, **60**, 309.
56 K. S. W. Sing, D. H. Everett, R. A. Haul, L. Moscou, R. A. Pirroti, J. Rouquerol and T. Siemieniewska, *Pure Appl. Chem.*, 1985, **57**, 603.
57 E. P. Barrett, L. G. Joyner and P. P. Halenda, *J. Am. Chem. Soc.*, 1951, **73**, 373.
58 S. Kahraman, M. Önal, Y. Sarikaya and I. Bozdogan, *Anal. Chim. Acta*, 2005, **552**, 201.
59 M. Popova, A. Ristić, K. Lazar, D. Maučec, M. Vassileva and N. Novak Tušar, *ChemCatChem*, 2013, **5**(4), 986.
60 M. Popova, A. Ristić, M. Mazaj, D. Maučec, M. Dimitrov and N. Novak Tušar, *ChemCatChem*, 2014, **6**, 271.
61 V. G. Deshmane and Y. G. Adewuyi, *Appl. Catal., A*, 2013, **462–463**, 196.
62 M. Akçay, *Appl. Catal., A*, 2005, **294**, 156.
63 F. Lónyi, J. Valyon, J. Engelhardt and F. Mizukami, *J. Catal.*, 1996, **160**, 279.
64 R. Barthos, F. Lónyi, J. Engelhardt and J. Valyon, *Top. Catal.*, 2000, **10**, 79.
65 V. L. C. Goncalves, B. P. Pinto, J. C. Silva and C. J. A. Mota, *Catal. Today*, 2008, **133–135**, 673.
66 Q.-H. Xia, K. Hidajat and S. Kawi, *J. Catal.*, 2002, **205**(2), 318.
67 S. Zhu, Y. Zhu, X. Gao, F. Dong, Y. Zhu, H. Zheng and Y. Li, *J. Catal.*, 2013, **306**, 155.
68 S. Zhu, Y. Zhu, X. Gao, T. Mo, Y. Zhu and Y. Li, *Bioresour. Technol.*, 2013, **130**, 45.
69 L. Wang, Q. Liu, M. Zhou and G. N. Xiao, *J. Nat. Gas Chem.*, 2012, **21**, 25.

